Afyon Kocatepe Üniversitesi Fen ve Mühendislik Bilimleri Dergisi

Afyon Kocatepe University Journal of Science and Engineering

AKÜ FEMÜBİD **21** (2021) 025603 (426-433) AKU J. Sci. Eng. **21** (2021) 025603 (426-433)

DOI: 10.35414/akufemubid.819348

Araştırma Makalesi / Research Article

An Analytical Study on Tsunami Run-up due to Submarine Landslides from Different Bottom Profiles

Baran AYDIN[1*]

[1] *Adana Alparslan Türkeş Science and Technology University, Faculty of Engineering, Department of Civil Engineering, Adana.*

**Corresponding author; e-mail: baydin@atu.edu.tr. ORCID ID: http://orcid.org/0000-0001-7838-3708*

Geliş Tarihi: 02.11.2020 Kabul Tarihi: 01.04.2021

Keywords

Submarine Landslides; Maximum Tsunami Run-up; Analytical Solution; Bottom Profile

Abstract

Tsunamis generated by submarine landslides were analyzed through a linear analytical model. Analytical solution existing in the literature was generalized to include different bottom profiles and maximum run-ups originating from two different bottom forcing functions, namely Gaussian wave and solitary wave cross sections were compared. Results indicated that the Gaussian cross section produces slightly larger maximum run-up than the solitary wave cross section, even if the two profiles had the same maximum vertical thickness initially and the area occupied by the former was less than the latter.

Farklı Taban Profiline Sahip Denizaltı Heyelanları Sonucu Meydana Gelen Tsunami Tırmanması için Analitik Bir Çalışma

Anahtar kelimeler

Denizaltı Heyelanları; Maksimum Tsunami Tırmanması; Analitik Çözüm; Taban Profili

Öz

Denizaltı heyelanlarının meydana getirdiği tsunamiler doğrusal bir analitik model aracılığıyla incelenmiştir. Literatürdeki çözüm farklı taban profillerini içerecek şekilde genelleştirilmiş ve kesiti Gauss ve soliter dalga olan taban profilleri sonucu oluşan maksimum tırmanmalar karşılaştırılmıştır. Sonuçlar, başlangıçta aynı kalınlığa sahip olmalarına ve Gauss profilinin kapladığı alanın daha az olmasına rağmen bu profilin oluşturduğu maksimum tırmanmanın daha fazla olduğunu göstermiştir.

1. Introduction

Underwater landslides are the second most common source of tsunamis after earthquakes (Gusiakov 2009). Yet, the coastal hazard posed by landslides is still underestimated. The remarkable 17 July 1998 Papua New Guinea (PNG) tsunami, with 2200 casualties and a maximum run-up of 15 m, was such a milestone event which drew scientists' interest to landslide tsunamis in the last two decades.

Modeling of landslide tsunamis is a challenging problem, both from physical and mathematical points of view. The sea floor is dynamic and hence the water depth is a function of time as well as space variables. The resulting partial differential equations governing propagation of the free surface disturbance are therefore nonhomogeneous or forced. For this reason, the number of studies attempting analytical solutions to subsequent modeling of landslide-generated tsunamis is limited, even in one horizontal dimension. The analytical solution proposed long ago by Tuck and Hwang (1972) was a remarkable contribution. They incorporated the sliding mass at the sea floor as a small time-dependent perturbation into the linear shallow-water wave equations and they quantified the resulting waves propagated offshore.

Tinti *et al.* (2001) started with the classical Euler equations for irrotational flow of an incompressible and inviscid fluid and first formulated, based on the shallow-water approximation, the general initial value problem for two dimensional propagation of tsunamis generated by rigid bodies sliding on the sea bottom. They then obtained the pattern and

calculated the energy of one dimensional waves propagating over a flat bottom by applying Duhamel's principle, a useful method for solving nonhomogeneous differential equations, and they also managed to provide results for a non-flat seafloor of a special type.

Liu *et al.* (2003) presented analytical solution through integral transform for the case of a Gaussian bottom forcing having a small vertical thickness compared to its horizontal length. They managed to provide, at least for a certain class of bottom disturbances, a generic form for the particular solution of the nonhomogeneous problem. They also compared their linear analytical solution with a nonlinear numerical solution and verified the analytical prediction of the maximum run-up as a function of beach slope over slide aspect ratio. Their study is revisited in the next section.

Di Risio and Sammarco (2003) presented an analytical model for generation of transient waves by fall of a block into water vertically, and validated their results from the linear theory with experiments. They showed that elevation of the leading wave generated by the landslide depends on slide length and energy through the impulse pressure released by the landslide at impact and that period of the generated wave depends on landslide length.

Trifunac *et al.* (2003) developed an analytical model to calculate near-field wave amplitudes originated from composite rectangular blocks moving horizontally with variable speed. Although providing good near-field estimations when slides moved with a velocity comparable to that of long waves, their results suggested that spatial distribution of the final uplift has to be considered for larger velocities.

Sammarco and Renzi (2008) employed an analytical model in two horizontal dimensions to study the wave field on a plane beach induced by a landslide at small times after the start of the motion. They also demonstrated differences in transient edge waves traveling along the shoreline at larger times with transient waves propagating over a bottom of constant depth and compared analytical results with experimental data. Shortly afterwards, Renzi and Sammarco (2010) modeled landslide tsunamis propagating around a conical island lying on a flat continental platform. They employed separation of variables and Laplace transform to solve the two wave problems, namely the problem in the constant-depth (outer) region and that in the variable-depth (inner) region and matched the solutions at the interface of the two regions to obtain the free-surface elevation, run-up and expression for the transient leading wave traveling offshore. Physical features of landslide tsunamis propagating in a round geometry are compared with those propagating along a straight coast and analytical results are also validated with experimental data.

Özeren and Postacıoğlu (2011) introduced a Green's function approach which proves to be useful for sources localized in space but extended in time and they applied it to calculate run-up of tsunamis triggered by submarine landslides.

In addition to the nondispersive models cited above, there are also few studies in the literature that analyze dispersion effects. Pelinovsky (2003) gave a short review of linear and nonlinear dispersive analytical models of tsunami wave generation by submarine landslides. Dutykh *et al.* (2011) presented a model for dispersive landslide motion along a curvilinear bottom, which takes into account the curvature effects of the sea bed, a feature that is usually neglected. Lo and Liu (2017) treated the problem of waves generated by a solid landslide moving at a constant speed in constant water depth, both in one- and two-dimensions and using both weakly and fully dispersive linear wave models. Besides providing a closed-form solution that can serve for benchmarking of numerical codes, they further examined the resonance solution and carried out convergence analysis.

On the other hand, as in the case of earthquake-generated tsunamis, stochastic methods for landslide-generated tsunamis as well are nowadays being employed in an effort to simulate the

subsequent waves more realistically. Ramadan *et al.* (2014) defined a two-dimensional stochastic submarine slide represented by the Heaviside (step) function under the influence of a Gaussian white noise process. Their results show that, the largest peak of the tsunami amplitude occurs when the bottom has spreading velocities that are equal to the tsunami velocity, and that the amplitude decreases due to dispersion as the tsunami departs away from the source. They also found that the mean amplitude is proportional with the propagation length and width of the stochastic source model and inversely proportional with the water depth.

Finally, significant contributions that helped in understanding the dynamics of the problem through either physical models constructed in laboratory scale (Watts 1998, Watts 2000, Fritz *et al.* 2004, Grilli and Watts 2005, Watts *et al.* 2005, Liu *et al.* 2005, Di Risio *et al.* 2009, Fuchs *et al.* 2013), numerical experiments through either commercial software or codes developed in-house (Lynett and Liu 2005, Perez *et al.* 2006, Ruffini *et al.* 2019) and several occasions of combination of physical and numerical models (Cecioni and Bellotti 2010, Montagna *et al.* 2011) should also be mentioned, although they are not the main focus of the present study.

What we focus on in this manuscript is the extension of Liu *et al.* (2003)'s solution to submarine landslides to provide further insight into their maximum run-up variation with beach slope, slide aspect ratio, and initial slide center. Hence, in the rest of the paper we first generalize the existing linear analytical solution to submarine landslides. We later propose a new of bottom profile with the same maximum thickness but different spatial distribution, calculate the associated particular solution and compare and discuss the results.

2. Analytical Model

We idealize the problem as a time-dependent bottom perturbation with a prescribed profile sliding on a constant slope in one dimension. Subsequent motion of surface waves generated by this mass can then be described by solving the so-called forced nonlinear shallow-water wave equations (Tuck and Hwang 1972)

$$(\eta^* - h^*)_{t^*} + [(h_0^* - h^* + \eta^*)u^*]_{x^*} = 0 \qquad (1a)$$

$$u_{t^*}^* + u^* u_{x^*}^* + \eta_{x^*}^* = 0 \qquad (1b)$$

In this set of dimensional equations, x^* is the horizontal space variable, t^* is time, $\eta^*(x^*, t^*)$ is the free surface height, $u^*(x^*, t^*)$ is the depth-averaged water velocity in the horizontal direction, and subscript letters indicate partial derivatives. $h_0^*(x^*) = x^* \tan\beta$ is the undisturbed water depth (β represents beach angle with the horizontal), and $h^*(x^*, t^*)$ is the time-dependent ocean floor forcing (Fig. 1). It should be noted that presence of h^* results in the nonhomogeneous term $h_{t^*}^*$ in eq.(1a). After introducing δ and L as the maximum vertical thickness and the maximum horizontal extent of the initial slide profile, the scaled variables can be defined as $x = x^*/L$, $\{\eta, h_0, h\} = \{\eta^*, h_0^*, h^*\}/\delta$, $u = u^*/\sqrt{g\delta}$, and $t = t^*/\sqrt{L^2/(g\delta)}$. Further assuming $\{\eta, h\} \ll h_0$ and $u \ll \sqrt{gh_0}$ (Tuck and Hwang 1972), the dimensional equations above can be linearized and combined into (Liu *et al.* 2003):

$$\eta_{tt} - \frac{\tan\beta}{\mu}(x\eta_x)_x = h_{tt} \qquad (2)$$

in which μ is the slide mass ratio (i.e. $\mu = \delta/L$). The initial conditions necessary for a unique solution of eq.(2) can be prescribed as an undisturbed initial sea surface ($\eta \equiv 0$) with zero initial velocity ($u \equiv 0$):

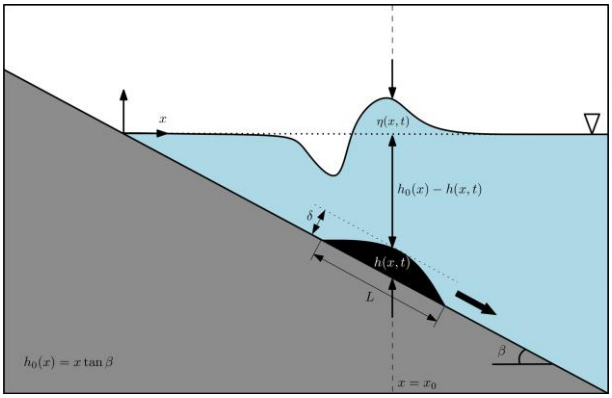

Figure 1. Definition sketch for the landslide problem (not to scale). x_0 is the x-coordinate of the slide submergence, while δ and L respectively indicate the maximum vertical

thickness and the maximum horizontal extent of the slide, at its initial location.

$$\eta(x,0)=0,\ \ \eta_t(x,0)=h_t(x,0) \tag{3}$$

Restricting to cases $\mu \ll 1$ so that $(\tan\beta)/\mu \sim O(1)$, Liu *et al.* (2003) proposed an analytical solution for the initial value problem defined by eqs.(2)-(3). They first introduced the change of variables

$$\xi = 2\sqrt{\frac{\mu}{\tan\beta}x} \tag{4}$$

through which eq.(2) transforms into

$$\eta_{tt} - \frac{1}{\xi}(\xi\eta_\xi)_\xi = h_{tt} \tag{5}$$

They then solved the nonhomogeneous eq.(5) with the help of Hankel (Fourier-Bessel) integral transform for

$$h(\xi,t) = e^{-(\xi-t)^2} \tag{6}$$

which is a subaerial seafloor deformation of Gaussian type. Their solution is revisited here for future reference: the homogeneous solution given by

$$\eta_h(\xi,t) = \int_0^\infty w[A\cos(wt) + B\sin(wt)]\,J_0(w\xi)dw$$

with coefficients $A(w)$ and $B(w)$ to be found from the initial conditions given in eqs.(3), is complemented by the particular solution

$$\eta_p(\xi,t) = \tfrac{1}{3}[h(\xi,t) - \xi h_\xi(\xi,t)] \tag{7}$$

together forming the complete solution of eq.(5) as $\eta(\xi,t) = \eta_h(\xi,t) + \eta_p(\xi,t)$, as expected.

We should remark here that the way Liu *et al.* (2003) acquired eq.(7) is particularly elegant and allows us to impose a variety of different bottom profiles, as presented in the next section. But we first extend the solution of Liu *et al.* (2003) so that it also employs submarine, in addition to subaerial, landslides.

2.1 Generalization of the Existing Analytical Model to Submarine Landslides

We suggest translation of the bottom disturbance by an amount $\xi_0 = 2\sqrt{\mu\, x_0/\tan\beta}$, i.e.

$$h_G(\xi,t) = e^{-(\xi-\xi_0-t)^2} \tag{8}$$

The advantage of defining the bottom profile as in eq.(8), which apparently satisfies eq.(7), is that the slide submergence parameter ξ_0 can be chosen in such a way that the sliding mass is completely submerged in the ocean initially, allowing analytical modeling of submarine landslides. We note that $\xi_0 = 0$ corresponds to the case of a subaerial slide, which partially starts outside of the sea.

Wave field generated by submarine landslides is analyzed and compared with the case of subaerial slides in the Results section. We now proceed with a new forcing function to be incorporated in eq.(5) and evaluate the associated particular solution.

2.2 New Bottom Profiles and Associated Particular Solutions

Here we first show that any forcing function $h(\xi,t)$ with the property

$$h_{\xi\xi}(\xi,t) = h_{tt}(\xi,t) \tag{9}$$

satisfies eq.(7) and hence becomes a particular solution of eq.(5). To verify this, we start writing the derivatives in eq.(7) explicitly:

$$\eta_{p,\xi} = -\frac{1}{3}\xi h_{\xi\xi}$$

$$\left(\xi\eta_{p,\xi}\right)_\xi = -\frac{1}{3}\left(2\xi h_{\xi\xi} + \xi^2 h_{\xi\xi\xi}\right)$$

$$\eta_{p,t} = -\frac{1}{3}(h_t - \xi h_{\xi t})$$

$$\eta_{p,tt} = -\frac{1}{3}(h_{tt} - \xi h_{\xi tt})$$

where we have omitted the arguments of the functions for ease of notation. Substitution into eq.(5) gives

$$\frac{1}{3}\left(h_{tt} - \xi h_{\xi tt}\right) + \frac{1}{3}\left(2h_{\xi\xi} + \xi h_{\xi\xi\xi}\right) = h_{tt}$$

which becomes an identity whenever eq.(9) is valid. This makes eq.(7) a particular solution of eq.(5) for any function $h(\xi,t)$ with the property given in eq.(9), i.e. $h_{\xi\xi}=h_{tt}$.

An immediate consequence of eq.(9) is that expression for the bottom disturbance is not limited to a Gaussian bottom forcing as per Liu *et al.* (2003), but a variety of more general profiles can be defined, with particular solutions given by eq.(7). In particular, any functional form

$$f(\xi,t)=F(\xi-a-t)$$

where a is constant will satisfy eq.(9) and hence will be a good candidate for a particular solution of eq.(5).

2.3 Solitary Bottom Profile

As a bottom profile alternative to eq.(8) we consider

$$h_S(\xi,t)=\operatorname{sech}^2(\xi-\xi_0-t) \qquad (10)$$

Fig. 2 compares the two forcing functions, h_G and h_S. The cross sections of the two profiles are very similar when they are plotted for the same parameter set. The solitary profile, however, is wider and it occupies more area than the Gaussian profile.

To show that h_S is a particular solution of eq.(5) we denote

$$T(\xi,t)=\tanh(\xi-\xi_0-t)$$

Omitting arguments for ease of notation, partial derivatives of h_S lead

$$h_{S,\xi}=-2h_ST, \quad h_{S,\xi\xi}=-2h_S(h_S-2T^2)$$

$$h_{S,t}=-h_{S,\xi}, \qquad h_{S,tt}=h_{S,\xi\xi}$$

$$h_{S,\xi t}=-h_{S,\xi\xi}, \quad h_{S,\xi\xi\xi}=8h_ST(2h_S-T^2)$$

Now, substituting h_S and its derivatives into eq.(7), we get

$$\eta_{p,\xi}=\frac{2}{3}\xi h_S(h_S-2T^2)$$

$$\left(\xi\eta_{p,\xi}\right)_\xi=\frac{4}{3}\xi h_S[h_S-2T^2-2\xi T(2h_S-T^2)]$$

$$\eta_{p,t}=\frac{2}{3}h_S[T-\xi(h_S-2T^2)]$$

$$\eta_{p,tt}=-\frac{2}{3}h_S[h_S-2T^2-4\xi T(2h_S-T^2)]$$

which can eventually be shown to satisfy eq.(5).

In the next section we compared the maximum tsunami run-ups produced by the new solitary bottom profile, eq.(10), with the Gaussian profile of Liu *et al.* (2003), eq.(8), for different values of the aspect ratio (μ) and initial submergence (ξ_0) of the slide.

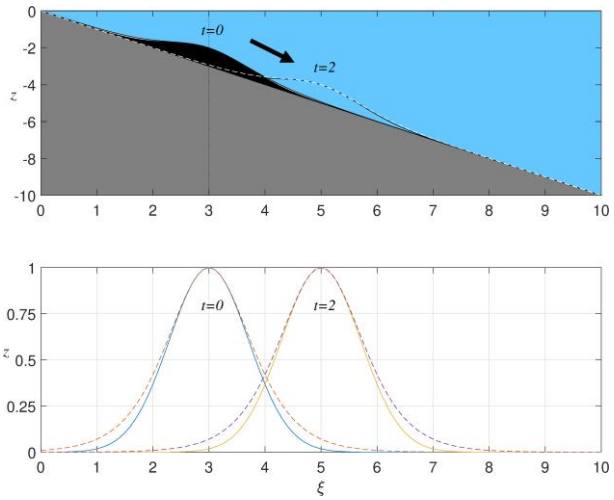

Figure 2. Gaussian bottom profile (solid line) defined in eq.(8) and solitary bottom profile (dashed line) defined in eq.(10) are indicated **(top)** over the slope, **(bottom)** over a horizontal axis, at two different instants for $\xi_0=3$.

3. Results

For the sake of a clear presentation of the results, geometrical parameters used in calculations are listed in Table 1 and our findings based on calculations with these parameters are summarized in the following.

Our calculations for the Gaussian bottom profile (h_G) showed that submarine slides generate greater waves at the shoreline when compared with subaerial slides (Fig. 3).

Results for subaerial slides (i.e. $\xi_0=0$) suggested that the maximum tsunami run-up defined by

$$R_{\max} = \max\{R(t), t \geq 0\}$$

Table 1. Values of the parameters used in calculations. Note that dimensional slide submergence in x-coordinate is $x_0^* = L(\xi_0^2/4)(\tan\beta)/\mu$, which depends on the following parameters: ξ_0 (dimensionless slide submergence in ξ-coordinate), β (beach angle with the horizontal), μ (slide aspect ratio), and δ (maximum slide thickness, fixed to 10 m in the calculations).

ξ_0	μ	β (°)	$\frac{\tan\beta}{\mu}$	L (m)	x_0^* (m)
1.5	0.1	5	0.87	100	49.21
1.5	0.15	5	0.58	66.67	21.87
1.5	0.2	5	0.44	50	12.30
3	0.1	5	0.87	100	196.85
3	0.15	5	0.58	66.67	87.49
3	0.2	5	0.44	50	49.21
6	0.1	5	0.87	100	787.40
6	0.15	5	0.58	66.67	349.95
6	0.2	5	0.44	50	196.85
1.5	0.1	10	1.76	100	99.18
1.5	0.15	10	1.18	66.67	44.08
1.5	0.2	10	0.88	50	24.80
3	0.1	10	1.76	100	396.74
3	0.15	10	1.18	66.67	176.33
3	0.2	10	0.88	50	99.18
6	0.1	10	1.76	100	1586.94
6	0.15	10	1.18	66.67	705.31
6	0.2	10	0.88	50	396.74

remains invariant with the slide aspect ratio μ, having a dimensionless value of $R_{\max} \approx 0.27$.

Besides, no wave receding was observed in this case, i.e. the run-up function assumed nonnegative values, $R(t) \geq 0$. The effect of the slide geometry on the maximum run-up is a translation: for larger μ (i.e. for steeper slide) the shoreline receives the maximum wave earlier (Figs. 3 and 4, top panels).

For submarine slides (i.e. $\xi_0 > 0$), on the other hand, $R_{\max}$ increased with μ within the same parameter range. A simple curve fitting procedure performed in MATLAB R2019a (a registered trademark of the Mathworks Inc.) suggested a relationship of the form

$$R_{\max} = a\ln\mu + b \qquad (11)$$

(see the lower panel of Fig. 3). Moreover, in this case, the shoreline experienced a significant wave receding before waves attacked and gave rise to the maximum run-up. The minimum run-down in magnitude was greater than the maximum run-up and the run-up curve as a function of time became steeper as μ increases, implying a decrease in the time interval between the minimum run-down and the maximum run-up (top panel of Fig. 3 and Fig. 4).

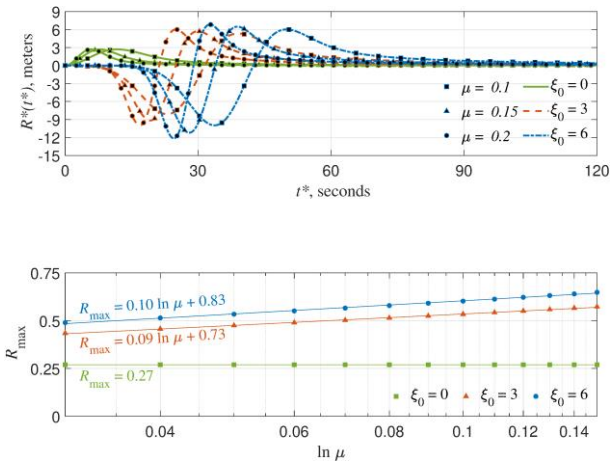

Figure 3. Comparison of run-up regimes for subaerial and submarine landslides. **(top)** Dimensional wave run-up as a function of dimensional time for three different values of the slide aspect ratio ($\mu = 0.1, 0.15, 0.2$) and the slide submergence ($\xi_0 = 0, 3, 6$). **(bottom)** Variation of dimensionless maximum run-up with μ. The models $R_{\max} = a\ln\mu + b$ shown in the lower panel are obtained through a curve fitting procedure performed in MATLAB R2019a (a registered trademark of the Mathworks Inc.), with coefficients of determination (R^2) greater than 0.99. The beach angle is $\beta = 10°$ and the maximum slide thickness is $\delta = 10$ m. Corresponding slide submergences (x_0^*) are tabulated in Table 1.

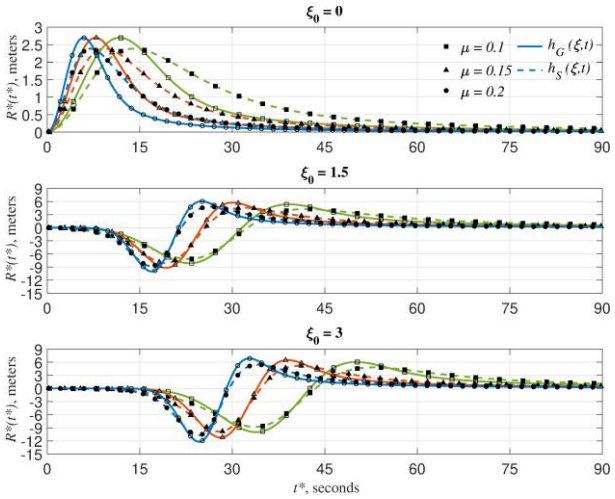

Figure 4. Comparison of run-up regimes for Gaussian (solid lines) and solitary bottom profiles (broken lines) for three different values of the slide aspect ratio ($\mu = 0.1, 0.15, 0.2$) and the slide submergence ($\xi_0 = 0, 1.5, 3$), respectively from top to bottom. The beach slope is $\beta = 5°$ and the maximum slide thickness is $\delta = 10$ m.

Corresponding dimensional slide submergences (x_0^*) are tabulated in Table 1.

In Fig. 4 we plotted time series of run-up for the two different bottom profiles having the same maximum thickness (Recall that Fig. 2 depicted a graphical comparison of the profiles). Calculations revealed that the run-up curves for both bottom profiles exhibit similar characteristics. Nevertheless, the Gaussian profile has a more confined run-up curve compared with that of the solitary profile, which exhibited a slower decay to zero as $t \to \infty$.

Interestingly, the confined exponential profile h_G given in eq.(8) generated greater maximum run-up (and also greater minimum run-down) compared with the hyperbolic profile h_S given in eq.(10), even if the cross-sectional area occupied by the Gaussian profile was less than that of the solitary profile. This difference became more significant as ξ_0 increases.

In accordance with our findings with the Gaussian profile above, the maximum wave run-up was independent of the slide aspect ratio parameter (μ) when the solitary slide is subaerial, while it increased with μ for submarine landslides.

4. Conclusions

In this study we compared run-up of tsunamis generated by underwater landslides for different cross sections of the sliding mass. We first extended the linear analytical solution of Liu *et al.* (2003) to employ submarine landslides with different bottom forcing functions as well. We then compared the maximum run-ups of two different bottom profiles, namely the Gaussian cross section originally suggested by Liu *et al.* (2003) and a new profile introduced here having the cross section of a solitary wave, i.e. hyperbolic secant.

The analytical model results obtained for subaerial and submarine landslides implied that the latter generate greater waves at the shoreline, compared to the former. In addition, the maximum run-up from subaerial slides did not change with the slide aspect ratio μ, while a linear increase was observed with $\ln \mu$ in the case of submarine landslides.

A comparison of bottom profiles indicated that the maximum run-up (minimum run-down) resulting from the Gaussian bottom profile is slightly larger than the maximum run-up (minimum run-down) of the waves originating from the solitary bottom forcing and that the difference becomes more significant when the slide is displaced from a deeper point in the ocean.

5. References

Cecioni, C. and Bellotti, G., 2010. Inclusion of landslide tsunamis generation into a depth integrated wave model. *Natural Hazards and Earth System Sciences*, **10**, 2259–2268.

Di Risio, M., Bellotti, G., Panizzo, A. and Girolamo, P. D., 2009. Three-dimensional experiments on landslide generated waves at a sloping coast. *Coastal Engineering*, **56(5)**, 659–671.

Di Risio, M. and Sammarco, P., 2008. Analytical modeling of landslide-generated waves. *Journal of Waterway, Port, Coastal, and Ocean Engineering*, **134**, 53–60.

Dutykh, D., Mitsotakis, D., Beysel, S. and Shokina, N., 2011. Dispersive waves generated by an underwater landslide. In: Numerical Methods for Hyperbolic Equations Theory and Applications, University of Santiago de Compostela, 245-250.

Fritz, H. M., Hager, W. H. and Minor, H.-E., 2004. Near field characteristics of landslide generated impulse waves. *Journal of Waterway, Port, Coastal, and Ocean Engineering*, **130(6)**, 287–302.

Fuchs, H., Winz, E. and Hager, W. H., 2013. Underwater landslide characteristics from 2D laboratory modeling. *Journal of Waterway, Port, Coastal, and Ocean Engineering*, **139(6)**, 480–488.

Grilli, S. T. and Watts, P., 2005. Tsunami generation by submarine mass failure I: Modeling, experimental validation, and sensitivity analyses. *Journal of Waterway, Port, Coastal, and Ocean Engineering*, **131(6)**, 283–297.

Gusiakov, V. K., 2009. Tsunami History: Recorded. In: The Sea, Volume 15: Tsunamis, Harvard University Press, 23-53.

Liu, P. L.-F., Lynett, P. and Synolakis, C. E., 2013. Analytical solutions for forced long waves on a sloping beach. *Journal of Fluid Mechanics*, **478**, 101–109.

Liu, P. L.-F., Wu, T.-R., Raichlen, F., Synolakis, C. E. and Borrero, J. C., 2005. Runup and rundown generated by three-dimensional sliding masses. *Journal of Fluid Mechanics*, **536**, 107–144.

Lo, H.-Y. and Liu, P. L.-F., 2017. On the analytical solutions for water waves generated by a prescribed landslide. *Journal of Fluid Mechanics*, **821**, 85–116.

Lynett, P. and Liu, P. L.-F., 2005. A numerical study of the run-up generated by three-dimensional landslides. *Journal of Geophysical Research: Oceans*, **110**, C03006.

Montagna, F., Bellotti, G. and Di Risio, M., 2011. 3D numerical modeling of landslide-generated tsunamis around a conical island. *Natural Hazards*, **58**, 591–608.

Özeren, S. and Postacıoğlu, N., 2011. Nonlinear landslide tsunami run-up. *Journal of Fluid Mechanics*, **691**, 440–460.

Pelinovsky, E. N., 2003. Analytical models of tsunami generation by submarine landslides. In: Submarine Landslides and Tsunamis, A. C. Yalçıner, E. N. Pelinovsky, E. Okal and C. E. Synolakis (Editors), Kluwer Academic Publishers, 111-128.

Perez, G., Garcia-Navarro, P. and Vazquez-Cendon, M. E., 2006. One-dimensional model of shallow water surface waves generated by landslides. *Journal of Hydraulic Engineering*, **132(5)**, 462–608.

Ramadan, K. T., Omar, M. A. and Allam, A. A., 2014. Modeling of tsunami generation and propagation under the effect of stochastic submarine landslides and slumps spreading in two orthogonal directions. *Ocean Engineering*, **75**, 90–111.

Renzi, E. and Sammarco, P., 2010. Landslide tsunamis propagating around a conical island. *Journal of Fluid Mechanics*, **650**, 251–285.

Ruffini, G., Heller, V. and Briganti, R., 2019. Numerical modelling of landslide-tsunami propagation in a wide range of idealised water body geometries. *Coastal Engineering*, **153**, 103518.

Sammarco, P. and Renzi, E., 2008. Landslide tsunamis propagating along a plane beach. *Journal of Fluid Mechanics*, **598**, 107–119.

Tinti, S., Bortolucci, E. and Chiavettieri, C., 2001. Tsunami excitation by submarine slides in shallow-water approximation. *Pure and Applied Geophysics*, **158**, 759–797.

Trifunac, M. D., Hayır, A. and Todorovska, M. I., 2003. A note on tsunami caused by submarine slides and slumps spreading in one dimension with nonuniform displacement amplitudes. *Soil Dynamics and Earthquake Engineering*, **23**, 223–234.

Tuck, E. O. and Hwang, L. S., 1972. Long wave generation on a sloping beach. *Journal of Fluid Mechanics*, **51**, 449–461.

Watts, P., 1998. Wavemaker curves for tsunamis generated by underwater landslides. *Journal of Waterway, Port, Coastal, and Ocean Engineering*, **124(3)**, 127–137.

Watts, P., 2000. Tsunami features of solid block underwater landslides. *Journal of Waterway, Port, Coastal, and Ocean Engineering*, **126(3)**, 144–152.

Watts, P., Grilli, S. T., Tappin, D. R. and Fryer, G. J., 2005. Tsunami generation by submarine mass failure II: Predictive equations and case studies. *Journal of Waterway, Port, Coastal, and Ocean Engineering*, **131(6)**, 298–310.